

Cite this: *RSC Adv.*, 2017, 7, 47104Received 6th September 2017  
Accepted 29th September 2017

DOI: 10.1039/c7ra09947a

rsc.li/rsc-advances

# Poly(*o*-aminothiophenol)-stabilized Pd nanoparticles as efficient heterogenous catalysts for Suzuki cross-coupling reactions

Yuan Chen,<sup>ab</sup> Minggui Wang,<sup>b</sup> Long Zhang,<sup>ab</sup> Yan Liu<sup>b</sup> and Jie Han<sup>ID</sup> <sup>\*b</sup>

Poly(*o*-aminothiophenol) (PATP)-stabilized Pd nanoparticles with Pd nanoparticles embedded in a polymer matrix have been obtained through a facile one-step route by mixing *o*-aminothiophenol monomer and Pd(NO<sub>3</sub>)<sub>2</sub> in an acidic aqueous solution without additional template or surfactant. The redox reaction between *o*-aminothiophenol and Pd(NO<sub>3</sub>)<sub>2</sub> leads to the simultaneous formation of a PATP polymer and Pd nanoparticles. The PATP-stabilized Pd nanoparticles have been characterized by TEM, FTIR, XRD, ICP-MS and XPS. Catalytic results showed that PATP-stabilized Pd nanoparticles were highly stable and active catalysts for Suzuki cross-coupling reactions, where high yields could be achieved with arylboronic acid and aryl halides bearing a variety of substituents.

## Introduction

Among the carbon–carbon bond formation reactions catalyzed by palladium (Pd) in organic synthesis,<sup>1–3</sup> cross-coupling reactions as simple and practical reactions<sup>4–6</sup> include the reactions of halogenated hydrocarbons with organotin (Stille reactions),<sup>7</sup> organoboron (Suzuki reactions),<sup>8</sup> organosilicon (Hiyama reactions),<sup>9</sup> alkenes (Heck reactions)<sup>10</sup> and alkynes (Sonogashira reactions).<sup>11</sup> The Suzuki cross-coupling reaction refers to the reaction between a halogenated hydrocarbon and an organic boron reagent catalyzed by Pd, and the reaction conditions are relatively mild, which is one of the important methods for preparing the asymmetric biphenyl compounds.<sup>12</sup> Since the use of organic boron reagents with low toxicity, high stability and easy preparation, the Suzuki cross-coupling reactions catalyzed by Pd are widely used and have attracted much attention due to the simple synthesis method and the easy recovery of the catalysts.<sup>13–16</sup> It is important to make use of inexpensive, safe and pollution-free reaction media in current organic synthesis. Early Beletskaya<sup>17</sup> reported the Suzuki coupling reactions of water-soluble iodobenzene and bromobenzene catalyzed by Pd(OAc)<sub>2</sub> and PdCl<sub>2</sub> respectively, which were carried out under the protection of inert gas and at room temperature. Later, Davydov<sup>18</sup> studied the reduction coupling reactions of water-insoluble aryl halides catalyzed by PdCl<sub>2</sub> and water-soluble triphenylphosphine in the emulsion, where the conversion of the aryl halides is still lower, less than 50%, and only the aryl iodide and bromide can be used as substrates. Chlorobenzene is an

ideal raw material for Suzuki cross-coupling reactions compared to bromobenzene and iodobenzene. However, it is greatly limited in practical production and applications due to the low reactivity of chlorobenzene. Therefore, it is highly desirable to develop efficient catalysts for the Suzuki cross-coupling reaction of chlorobenzene. We have successfully prepared the poly(*o*-aminothiophenol) (PATP)-stabilized gold nanoparticles as catalysts for the Suzuki cross-coupling reactions of aryl halides with arylboronic acids in water.<sup>19</sup> In order to further expand the research scope of substrates and improve the yield of the products, PATP-stabilized Pd nanoparticles were chosen as catalysts for the Suzuki cross-coupling reactions of aryl halides with arylboronic acids in water, especially aryl chlorides with low reactivity. The results showed that PATP-stabilized Pd nanoparticles can effectively promote the Suzuki cross-coupling reactions of aryl halides with arylboronic acids to obtain the series of diaryl compounds with high yields.

## Experimental

### Materials

*o*-Aminothiophenol (ABCR GmbH & Co. KG) was distilled under reduced pressure before use. All other reagents were of analytical grade and purchased from Alfa Aesar. The water used in this study was deionized by milli-Q Plus system (Millipore, France), having 18.2 MΩ electrical resistivity.

### Preparation of PATP-stabilized Pd nanoparticles

In a typical synthesis, *o*-aminothiophenol (100.0 mg) was dispersed in HCl aqueous solution (1.0 mol L<sup>−1</sup>, 20 mL) with magnetic stirring at room temperature to obtain a uniform solution. Then 4 mL palladium nitrate aqueous solution

<sup>a</sup>School of Animal Pharmaceuticals, Jiangsu Agri-animal Husbandry Vocational College, Taizhou 225300, Jiangsu, People's Republic of China

<sup>b</sup>School of Chemistry and Chemical Engineering, Yangzhou University, Yangzhou 225002, Jiangsu, People's Republic of China. E-mail: hanjie@yzu.edu.cn



(0.1 mol L<sup>-1</sup>) was added to the above mixture, stirring at room temperature for 6 h. Finally, the mixture was washed with deionized water and sodium hydroxide aqueous solution for several times and the resulting products were diluted by deionized water to a certain concentration, and then placed at room temperature and under normal pressure for further use. In order to reveal the effect of molar ratio between *o*-aminothiophenol monomer and palladium nitrate, the amount of *o*-aminothiophenol was decreased to 50 mg and 25 mg while maintaining other conditions unchanged.

### Catalysis for Suzuki cross-coupling reactions

Aryl halide (2.0 mmol), phenylboronic acid (2.4 mmol) and NaOH (8.0 mmol) were added to 40 mL deionized water, which were stirred at 80 °C until the above-mentioned substances were completely dissolved. Then a certain amount of Pd catalysts (0.08 mol%) was added to the mixed solution, and the reaction mixture was stirred for 4 h. After the mixture was cooled to room temperature, the product was extracted three times with diethyl ether (3 × 20 mL), then the organic layer was dried with excessive Na<sub>2</sub>SO<sub>4</sub>. After filtration, volatile substances were removed under reduced pressure. The crude material was purified by flash chromatography on silica gel.

### Characterization

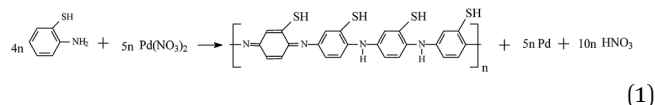
The morphologies of products were characterized by a transmission electron microscopy (TEM, Tecnai-12 Philip Apparatus Co., USA) and a high-resolution transmission electron microscopy (HR-TEM, JEOL, JEM-2010, Japan). FTIR spectra of products were recorded in the range of 400–4000 cm<sup>-1</sup> using FTIR spectroscopy (Nicolet-740, USA) and the samples were prepared in pellet form with spectroscopic grade KBr. X-ray diffraction (XRD) patterns were recorded by an X-ray diffractometer (XRD, MO3XHF22, MacScience, Japan) and X-ray photoelectron spectroscopy (XPS) data were recorded by a X-ray photoelectron spectrometer (Thermo Escalab 250, USA). The content of Pd was measured by inductively coupled plasma mass spectrometry (ICP-MS, ELAN DRC-e, PE, USA) analysis. Gas chromatography (GC) analysis (6890N, Agilent, USA) was performed on an Agilent DB-1 GC-FID system equipped with a 100% dimethyl polysiloxane capillary column (length, 30 m; internal diameter, 0.25 mm; film thickness, 0.25 μm). The GC yield was obtained from the calibration curve.

## Results and discussion

### Morphology and structure of PATP-stabilized Pd nanoparticles

The chemical oxidation polymerization of *o*-aminothiophenol monomers to PATP polymer is induced by the reduction of Pd(II) to Pd(0), where PATP polymer and Pd nanoparticles are generated simultaneously (eqn (1)), resulting in the formation of PATP-stabilized Pd nanoparticles.<sup>20–22</sup> The PATP polymer oligomers prefer to locate on surfaces of newly formed Pd nuclei to lower down the surface energy. The choice of *o*-aminothiophenol as the reductant is based on the fact that its

polymerized polymer PATP can act as effective capping agent for Pd nanoparticles as conjugated  $\pi$  electrons of benzene rings and thiol groups coexist in PATP chains which can significantly control and stabilize Pd nanoparticles.<sup>23</sup> As a consequence, in the obtained PATP-stabilized Pd nanoparticles, Pd nanoparticles are always embedded in polymer matrix.



The prepared PATP-stabilized Pd nanoparticles was centrifuged and then the Pd content of the supernatant solution was measured to be 0.0084% of the total Pd content through ICP-MS analysis, indicating that Pd ions were almost completely reduced in the process. As a result, the amount of Pd in the product was considered to be equal to that in initial addition of Pd(NO<sub>3</sub>)<sub>2</sub>. Fig. 1 shows the TEM images of PATP-stabilized Pd nanoparticles, where the dark dots as ascribed to Pd nanoparticles are well dispersed in PATP polymer matrix. Fig. 1A is the freshly prepared PATP-stabilized Pd nanoparticles, where Pd nanoparticles are about 1 nm in diameter without aggregation (Fig. 1B). The clear lattice fringes 0.223 nm as shown in insert in Fig. 1B that attributed to the (111) plane of face-centered cubic (fcc) Pd<sup>24</sup> indicates the signal crystal of each Pd nanoparticles. Further investigations revealed that the molar ratio between *o*-aminothiophenol monomer and palladium nitrate has negligible effect on the size of Pd nanoparticles, which should be ascribed to the effective capping ability of polymerized polymer PATP for Pd nanoparticles. Compared to

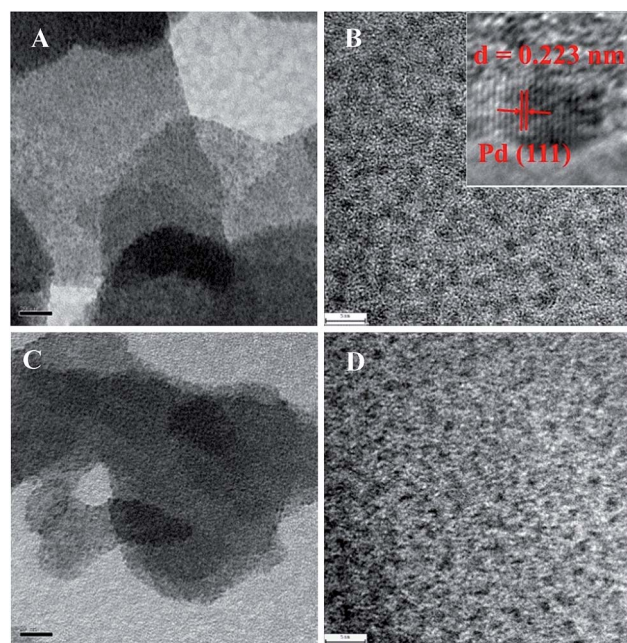


Fig. 1 TEM images of PATP-stabilized Pd nanoparticles: (A and C) freshly prepared sample, (C and D) after aging 6 months. Scale bar: (A and C) 20 nm, (B and D) 5 nm.



the freshly prepared Pd nanoparticles, the size of Pd nanoparticles after aging 6 months at room temperature does not change (Fig. 1C and D), which shows that PATP polymer plays the role of protective agent to prevent the aggregation of Pd nanoparticles.

As shown in Fig. 2A, the strong absorption band at 3150–3500  $\text{cm}^{-1}$  can be ascribed to the N–H stretching vibrations, the weak absorption band at 2615  $\text{cm}^{-1}$  is attributed to the S–H stretching vibrations. The strong characteristic peaks at 1609  $\text{cm}^{-1}$  and 1475  $\text{cm}^{-1}$  come from the C=C stretching deformation of quinone and benzene, respectively, where the relative intensity of the former is weaker than that of the latter,

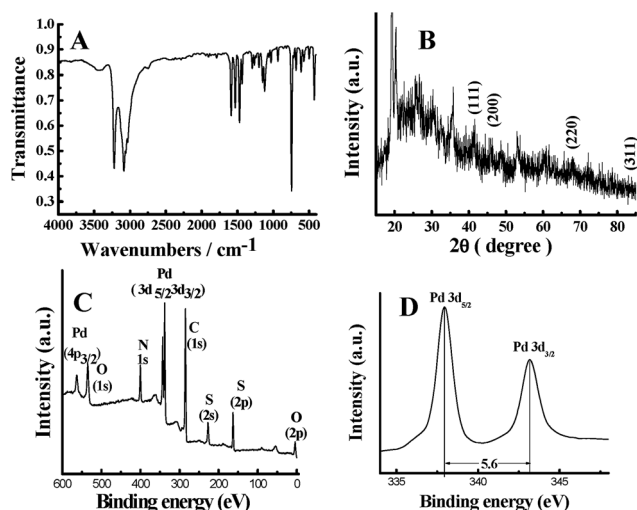


Fig. 2 (A) FTIR, (B) XRD, and (C and D) XPS spectra of PATP-stabilized Pd nanoparticles.

Table 1 Effect of catalyst amount, alkali and solvent on the yield of Suzuki cross-coupling of chlorobenzene and benzoboric acid<sup>a</sup>

<chem>c1ccccc1Cl</chem> + <chem>c1ccccc1B(O)O</chem> $\xrightarrow[\text{alkali (4 equiv), solvent, 80 }^\circ\text{C, 4 h}]{\text{Pd catalysts (n mol\%)}}$ <chem>c1ccccc1-c2ccccc2</chem>				
Entry	Pd amount (n mol%)	Solvent	Alkali	Yield (%)
1	0.06	H <sub>2</sub> O	NaOH	94
2	0.08	H <sub>2</sub> O	NaOH	96
3	0.10	H <sub>2</sub> O	NaOH	96
4	0.08	H <sub>2</sub> O	K <sub>2</sub> CO <sub>3</sub>	96
5	0.08	H <sub>2</sub> O	Na <sub>3</sub> PO <sub>3</sub>	95
6	0.08	H <sub>2</sub> O	Et <sub>3</sub> N	98
7	0.08	DMF/H <sub>2</sub> O (1 : 1)	NaOH	96
8	0.08	THF/H <sub>2</sub> O (1 : 1)	NaOH	95
9	0.08	C <sub>2</sub> H <sub>5</sub> OH/H <sub>2</sub> O (1 : 1)	NaOH	96
10	0.08	C <sub>2</sub> H <sub>5</sub> OH	NaOH	96
11	0.08	DMF	NaOH	10
12	0.08	THF	NaOH	6
13	0.08	TX-100/H <sub>2</sub> O (2%, w/w)	NaOH	97 <sup>b</sup>

<sup>a</sup> Chlorobenzene (2 mmol), benzoboric acid (2.4 mmol), 80  $^\circ\text{C}$ , 4 h.

<sup>b</sup> Reaction temperature was maintained at 50  $^\circ\text{C}$ .

Table 2 Suzuki cross-coupling of chlorobenzene and phenylboronic acid catalyzed by PATP-stabilized Pd nanoparticles<sup>a</sup>

<chem>c1ccccc1Cl</chem> + <chem>c1ccccc1B(O)O</chem> $\xrightarrow[\text{NaOH (4 equiv), H}_2\text{O, 80 }^\circ\text{C, 4 h}]{\text{Pd catalysts (0.08 mol\%)}}$ <chem>c1ccccc1-c2ccccc2</chem>		
No.	Storage time (day)	Yield (%)
1	1	96
2	10	96
3	30	95
4	180	95

<sup>a</sup> Chlorobenzene (2 mmol), phenylboronic acid (2.4 mmol), Pd catalyst (0.08%), NaOH (8 mmol).

Table 3 Recovery and reuse of PATP-stabilized Pd nanoparticles as catalysts for Suzuki cross-coupling of chlorobenzene and phenylboronic acid<sup>a</sup>

<chem>c1ccccc1Cl</chem> + <chem>c1ccccc1B(O)O</chem> $\xrightarrow[\text{NaOH (4 equiv), H}_2\text{O, 80 }^\circ\text{C, 4 h}]{\text{Pd catalysts (0.08 mol\%)}}$ <chem>c1ccccc1-c2ccccc2</chem>						
Use	1st	2nd	3rd	4th	5th	6th
Yield (%)	96	96	96	95	95	96

<sup>a</sup> Chlorobenzene (2 mmol), phenylboronic acid (2.4 mmol), Pd catalyst (0.08%), NaOH (8 mmol).

indicating the amount of quinone ring is less than that of benzene ring. From the XRD pattern of PATP-stabilized Pd nanoparticles (Fig. 2B), it can be seen that the crystal structure of Pd nanoparticles is face-centered cubic, which is consistent with the previous report.<sup>25</sup> The main diffraction peaks of PATP-stabilized Pd nanoparticles appearing at 40.1 $^\circ$ , 46.4 $^\circ$ , 68.1 $^\circ$  and 82.1 $^\circ$  that corresponding to (111), (200), (220) and (311) Bragg planes of Pd,<sup>26</sup> can be observed. The broad diffraction peaks between 15–35 $^\circ$  indicate the amorphous structure of PATP polymer.

The XPS spectrum shows clearly the signatures of C, N and S for PATP, and Pd for Pd nanoparticles (Fig. 2C). Fig. 2D represents the XPS signature of the Pd 3d, with the splitting of 5.6 eV

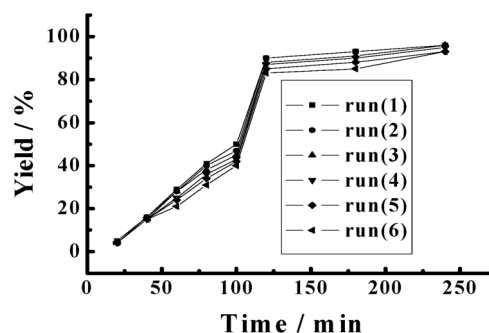
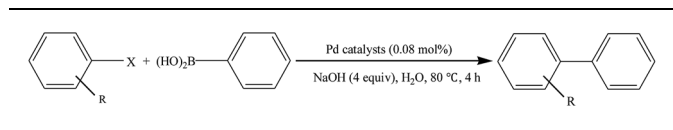


Fig. 3 Dependence of biphenyl yield on reaction time for the Suzuki cross-coupling of chlorobenzene and phenylboronic acid catalyzed by PATP-stabilized Pd nanoparticles under different runs.

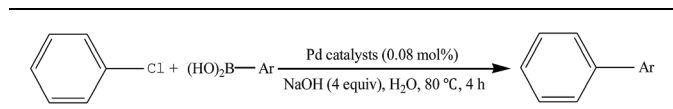


**Table 4** Suzuki cross-coupling of aryl halides and phenylboronic acids<sup>a</sup>

Entry	X	R	Yield (%)
1	Br	H	99
2	I	H	100
3	Cl	2-OCH <sub>3</sub>	95
4	Cl	4-OCH <sub>3</sub>	95
5	Cl	4-CHO	97
6	Cl	4-COOH	97

<sup>a</sup> Aryl halides (2 mmol), phenylboronic acid (2.4 mmol), Pd catalyst (0.08%), NaOH (8 mmol).

indicating the metallic nature of Pd. However, the energy peak of Pd (3d<sub>5/2</sub>) at 337.1 eV is 1.9 eV higher than that of the standard Pd (3d<sub>5/2</sub>) at 335.2 eV, indicating the change of the chemical environment of Pd nanoparticles. The possible reason is that Pd nanoparticles may coordinate with other atoms and

**Table 5** Suzuki cross-coupling of chlorobenzene and arylboronic acids<sup>a</sup>

Entry	Arylboronic acid	Yield (%)
1		78
2		83
3		79
4		90
5		76
6		58
7		40

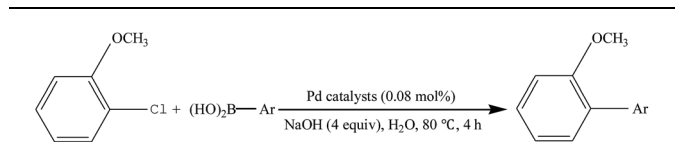
<sup>a</sup> Chlorobenzene (2 mmol), arylboronic acids (2.4 mmol), Pd catalyst (0.08%), NaOH (8 mmol).

loss of partial electrons, leading to the decrease of the electronic cloud density of the valence electrons and the shielding effect of the electrons in the inner shell layer, finally resulting in the increase of the binding energy of the inner shell layer. Results indicate compact interactions between PATP polymer and Pd nanoparticles.

### Catalysis in Suzuki cross-coupling reactions

The Suzuki cross-coupling reaction of aryl halides with arylboronic acids is one of the most powerful and convenient synthetic protocols for the generation of biaryl in organic chemistry.<sup>27</sup> Pd nanoparticles usually show enhanced reactivity under mild conditions because of their large surface area. Herein, the Suzuki cross-coupling reactions were then chosen as the target model reactions to test the catalytic performances of PATP-stabilized Pd nanoparticles.

Table 1 shows the synthetic conditions of catalyst amount, alkali and solvent on the biphenyl yield of Suzuki cross-coupling reaction of chlorobenzene and benzoboric acid. The optimized choice is using NaOH as the alkali (entries 2, 4–6, Table 1), H<sub>2</sub>O as the green solvent (entries 2, 7–13, Table 1), and 0.08 mol% Pd

**Table 6** Suzuki cross-coupling of 2-chloroanisole and arylboronic acids<sup>a</sup>

Entry	Arylboronic acid	Yield (%)
1		64
2		75
3		43
4		72
5		61
6		44
7		21

<sup>a</sup> 2-Chloroanisole (2 mmol), arylboronic acids (2.4 mmol), Pd catalyst (0.08%), NaOH (8 mmol).





catalysts (entries 1–3, Table 1), the yield can reach as high as 96%. It was found that when using pure organic solvents, such as THF and DMF, the yield is below 10% (entries 11, 12, Table 1). As the PATP polymer shows high solubility in such solvents, the dissolution of PATP in organic solvents leads to aggregation of supported Pd nanoparticles, which will eventually result in decreased catalytic activity. In addition, the introduction of surfactant in the reaction system can lower down the reaction temperature from 80 to 50 °C with comparable yield (entry 13). This is mainly related to the special property of surfactant, which can self-assemble into micelles that can increase the solubility of reactants (chlorobenzene and benzoic acid) in water. The concentration of reactants in micelles is favorable for catalytic reactions, ensuring high yield even at low reaction temperature.

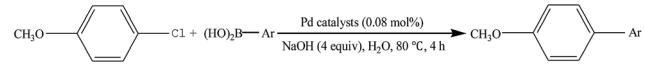
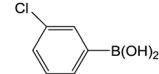
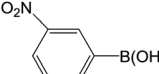
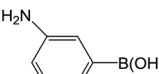
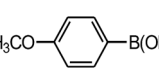
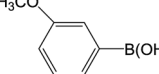
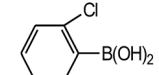
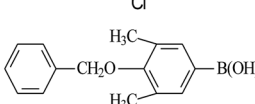
The effect of the aging time of catalyst on the yield of biphenyl was also investigated. As seen in Table 2, the yield of biphenyl which was produced by the Suzuki cross-coupling of chlorobenzene and phenylboronic acid catalyzed by the freshly prepared PATP-stabilized Pd nanoparticles was 96%. When the catalyst was aged for 6 months, the yield can also reach as high as 95%, which proved high stability and activity of the catalysts.

The recyclability of PATP-stabilized Pd nanoparticles as catalysts was also studied, where the used catalysts were

centrifuged, filtered and washed with water three times to remove the by-products adsorbed on the surfaces of catalysts, and then were reused for the repeated catalytic reaction under the same reaction conditions. The results showed that the yield of biphenyl almost unchanged (Table 3). The PATP-stabilized Pd nanoparticles as catalysts remained the same size after six cycles (Fig. 1), together with similar kinetic curves for each run (Fig. 3), which provided high recyclability of the catalysts. In addition, both the yield and recyclability of PATP-stabilized Pd nanoparticles are better than those using commercial Pt/C catalysts,<sup>28</sup> revealing their high potentials in Suzuki cross-coupling reactions.

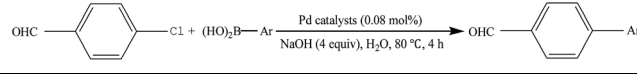
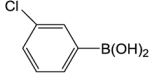
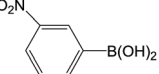
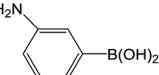
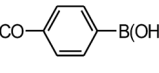
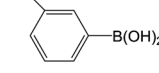
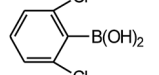
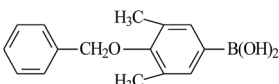
The yields of diaryl produced by the Suzuki cross-coupling of aryl halides and phenylboronic acids at the same reaction conditions were shown in Table 4. As for bromobenzene and iodobenzene, the yields of diaryl reached as high as 99% (entry 1) and 100% (entry 2), respectively. It is reasonable as the reactivity of aryl halides is in the following order: iodobenzene > bromobenzene > chlorobenzene. In addition, it can be seen that PATP-stabilized Pd nanoparticles can also be well suited for the Suzuki cross-coupling of chlorobenzene with various substituents and phenylboronic acids, where the yields were more than 95% (entries 3–6). Besides, when activated aryl chloride was used, the yields were higher (entry 5, 6, Table 4) than those of deactivated ones (entries 3, 4, Table 4).

**Table 7** Suzuki cross-coupling of 4-chloroanisole and arylboronic acid<sup>a</sup>

		
Entry	Arylboronic acid	Yield (%)
1		70
2		74
3		79
4		80
5		50
6		40
7		31

<sup>a</sup> 4-Chloroanisole (2 mmol), arylboronic acids (2.4 mmol), Pd catalyst (0.08%), NaOH (8 mmol).

**Table 8** Suzuki cross-coupling of 4-chlorobenzaldehyde and arylboronic acids<sup>a</sup>

		
Entry	Arylboronic acid	Yield (%)
1		83
2		85
3		81
4		88
5		77
6		61
7		40

<sup>a</sup> 4-Chlorobenzaldehyde (2 mmol), arylboronic acids (2.4 mmol), Pd catalyst (0.08%), NaOH (8 mmol).



Chlorobenzene is cheaper than bromobenzene and iodobenzene, but the use of aryl chlorides is limited by their weak reactivity. Therefore, searching suitable catalysts and reaction system for the Suzuki cross-coupling reactions of aryl chlorides have attracted increasing attention. As shown in Table 5, PATP-stabilized Pd nanoparticles can catalyze the Suzuki cross-coupling reactions of chlorobenzene and arylboronic acids (entries 1–5). The yields of *para*-substituted arylboronic acids (entry 4) were higher than those of *meta*-substituted arylboronic acids (entries 1–3, 5). The lower yields of entries 6 and 7 were 58% and 40%, respectively, owing to the obvious steric hindrance effect.<sup>29</sup>

The yields of the Suzuki cross-coupling of 2-chloroanisole and arylboronic acids are shown in Table 6. It can be seen that the yields were relatively low, and the yield of the Suzuki cross-coupling of 2-chloroanisole and phenylboronic acid even with an electron-withdrawing group was only 75% (entry 2). However, the yields were obviously affected by steric hindrances when phenylboronic acid with the same electron-donating group at different positions and the 4-substituted phenylboronic acid were preferred (entry 5 vs. 4).

The catalytic activity was further investigated to use 4-chloroanisole (Table 7). The results indicate that 4-chloroanisole is more suitable for the Suzuki cross-coupling

reactions than 2-chloroanisole (Tables 7 vs. 6) due to the steric hindrance effect.

Further investigations demonstrated that high yields could also be obtained when using 4-chlorobenzaldehyde (Table 8) and 4-chlorobenzoic acid (Table 9), respectively, where the steric hindrance effect plays the determining role in their activity. Therefore, the results indicate that the prepared PATP-stabilized Pd nanoparticles as catalysts are suitable for the Suzuki cross-coupling of chlorobenzene with different substituents and arylboronic acids, and the moderate yields can be obtained even for those substrates with larger steric hindrance (entries 6, 7, Tables 8 and 9).

## Conclusions

In summary, PATP-stabilized Pd nanoparticles with high stability have been successfully fabricated by the oxidation-reduction of *o*-aminothiophenol and Pd(NO<sub>3</sub>)<sub>2</sub>, where the PATP polymer can act as the stabilizer for Pd nanoparticles. The method of synthesis is simple and green, which does not require any external protective agent and additives. The prepared PATP-stabilized Pd nanoparticles exhibit excellent catalytic performance in Suzuki cross-coupling reactions of aryl halides and arylboronic acid, which prove their potential in catalysis.

## Conflicts of interest

There are no conflicts to declare.

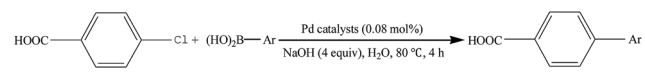
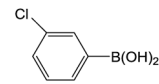
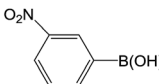
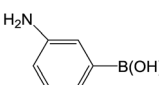
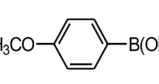
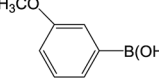
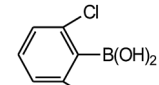
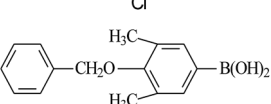
## Acknowledgements

The authors gratefully acknowledge financial support from the National Natural Science Foundation of China (21673202), Qing Lan Project, Priority Academic Program Development of Jiangsu Higher Education Institutions, Jiangsu Overseas Research & Training Program for University Prominent Young & Middle-aged Teachers and Presidents, Jiangsu High-end Research & Training Program for Professional Leaders of Higher Vocational Colleges (2016GRFX023), and the Phoenix Scholars Program of Jiangsu Agri-animal Husbandry Vocational College. We would also like to acknowledge the technical support received at the Testing Center of Yangzhou University.

## Notes and references

- 1 S. G. Newman and M. Lautens, *J. Am. Chem. Soc.*, 2011, **133**, 1778–1780.
- 2 M. K. Zhu, J. F. Zhao and T. P. Loh, *Org. Lett.*, 2011, **13**, 6308–6311.
- 3 T. Hamasaki, Y. Aoyama, J. Kawasaki, F. Kakiuchi and T. Kochi, *J. Am. Chem. Soc.*, 2015, **137**, 16163–16171.
- 4 Y. Shi, X. Li, J. Liu, W. Jiang and L. Sun, *Tetrahedron Lett.*, 2010, **51**, 3626–3628.
- 5 L. Goswami, P. Gogoi, J. Gogoi, A. Borah, M. R. Das and R. C. Boruah, *Tetrahedron Lett.*, 2014, **55**, 5539–5543.

Table 9 Suzuki cross-coupling of 4-chlorobenzoic acid and arylboronic acids<sup>a</sup>

		
Entry	Arylboronic acid	Yield (%)
1		81
2		85
3		80
4		88
5		78
6		60
7		57

<sup>a</sup> 4-Chlorobenzoic acid (2 mmol), arylboronic acids (2.4 mmol), Pd catalyst (0.08%), NaOH (8 mmol).



- 6 A. D. Burrows, L. C. Fisher, T. J. Mays, S. P. Rigby, S. E. Ashbrook and D. M. Dawson, *J. Organomet. Chem.*, 2015, **792**, 134–138.
- 7 J. Sun, X. Feng, Z. Zhao, Y. Yamamoto and M. Bao, *Tetrahedron*, 2014, **70**, 7166–7171.
- 8 F. R. Fortea-Pérez, I. Schlegel, M. Julve, D. Armentano, G. D. Munno and S.-E. Stiriba, *J. Org. Chem.*, 2013, **743**, 102–108.
- 9 H. Zhang, C. Wang, Z. Li and Z. Wang, *Tetrahedron Lett.*, 2015, **56**, 5371–5376.
- 10 J. Mondal, A. Moda and A. Bhaumik, *J. Mol. Catal. A: Chem.*, 2011, **350**, 40–48.
- 11 G. L. Gao, Y. N. Niu, Z. Y. Yan, H. L. Wang, G. W. Wang, A. Shaikat and Y. M. Liang, *J. Org. Chem.*, 2010, **75**, 1305–1308.
- 12 A. Chatterjee and T. R. Ward, *Catal. Today*, 2016, **146**, 820–840.
- 13 S. M. Chergui, A. Ledebt, F. Mammeri, F. Herbst, B. Carbonnier, H. B. Romdhane, M. Delamar and M. M. Chehimi, *Langmuir*, 2010, **26**, 16115–16121.
- 14 J. C. Park, E. Heo, A. Kim, M. Kim, K. H. Park and H. Song, *J. Phys. Chem. C*, 2011, **115**, 15772–15777.
- 15 G. A. Molander and I. Shin, *Org. Lett.*, 2013, **15**, 2534–2537.
- 16 B. D. Briggs, R. T. Pekarek and M. R. Knecht, *J. Phys. Chem. C*, 2014, **118**, 18543–18553.
- 17 N. A. Bumagin, V. V. Bykov and I. P. Beletskaya, *Russ. Chem. Bull.*, 1989, **38**, 2206.
- 18 D. V. Davydov and I. P. Beletskaya, *Russ. Chem. Bull.*, 1995, **44**, 1139–1140.
- 19 J. Han, Y. Liu and R. Guo, *J. Am. Chem. Soc.*, 2009, **131**, 2060–2061.
- 20 S. T. Selvan and M. Nogami, *J. Mater. Sci. Lett.*, 1998, **17**, 1385–1388.
- 21 M. C. Henry, C. C. Hsueh, B. P. Timko and M. S. Freund, *J. Electrochem. Soc.*, 2001, **148**, 155–162.
- 22 P. R. Selvakannan, S. Mandal, R. Pasricha and M. Sastry, *J. Colloid Interface Sci.*, 2004, **279**, 124–131.
- 23 J. Han, Y. Liu and R. Guo, *J. Am. Chem. Soc.*, 2009, **131**, 2060–2061.
- 24 Y. Liu, C. Wang, Y. Wei, L. Zhu, D. Li, J. S. Jiang, N. M. Markovic, V. R. Stamenkovic and S. Sun, *Nano Lett.*, 2011, **11**, 1614–1617.
- 25 Y. Wan, H. Wang, Q. Zhao, M. Klingstedt, O. Terasaki and D. Zhao, *J. Am. Chem. Soc.*, 2009, **131**, 4541–4550.
- 26 C. Damle, A. Kumar and M. Sastry, *J. Phys. Chem. B*, 2002, **106**, 297–302.
- 27 N. Miyaura and A. Suzuki, *Chem. Rev.*, 1995, **95**, 2457–2483.
- 28 M. Lysén and K. Köhler, *Synthesis*, 2006, 692–698.
- 29 Y. Chen, S. Lu, W. J. Liu and J. Han, *Colloid Polym. Sci.*, 2015, **293**, 2301–2309.

